

Simulation and Stability Analysis of Three-Phase Shunt Active Filter Based on Internal Model Controller (IMC)

Chegudi RangaRao^{1,2*}, R. Balamurugan¹ and RamaKoteswaraRao Alla¹

¹Department of Electrical Engineering, Annamalai University, Annamalai Nagar, Chidambaram, Tamilnadu-608002 India.

²Department of Electrical and Electronics Engineering, RVR &JC College of Engineering, Guntur, Andhra Pradesh-522019, India

Received 29 March 2021; Accepted 6 December 2021

Abstract

Three-phase Shunt Active Power Filter (SAPF) based on the Internal Model Controller (IMC) is designed for the reduction of harmonics generated by the non-linear load. The main motivation of the paper is to design an IMC controller for reduction of harmonics and also analyze the stability of SAPF using with and without IMC controller. In the past, passive filter techniques are applied to maintain the quality of the power within the limited recommended standard (IEEE-519). To overcome the drawbacks of a passive filter and conventional current controller, an IMC-based Shunt active filter is proposed for the harmonic reduction in the electrical distribution system. Furthermore, the stability of the system is ensured by using an internal model controller. The system performance has been analyzed in terms of Total Harmonic Distortion (THD) with and without compensation. From simulation results, it is clear that THD generated by the proposed IMC is within the recommended standard of IEEE-519 (5%). A complete system is modeled and verified by using MATLAB/Simulink.

Keywords: Shunt active filter, IMC, Stability Analysis, and THD performance.

1. Introduction

The power quality is one of the most significant issues in distributed power systems due to the involvement of the power converter topologies and should maintain the quality of the power is supplied to the customers [1]. The various power electronics conversion system is involved and due to these, harmonics can be generated. To limit harmonics generated by power electronics systems, various types of filters are utilized and it should be maintained by IEEE-519 standard limits [2]. In the past, passive filter techniques are applied to the power system for the reduction of harmonics generated by the non-linear loads [3]. Even though, the performance of the passive filters is not up to the mark due to the larger, resonance frequency variation, not adaptable for network parameters [4]. Nowadays, active filter techniques are applied to the distributed systems to limit the current harmonics generated by the non-linear loads. [5]. Furthermore, Shunt Active Power Filter (SAPF) solves the various problems of conventional techniques such as reduction of current harmonics and improvement of power factor as well [6]. In this paper, simulation and design features of Internal Model Controller (IMC) for the compensation of harmonics generated by the nonlinear load.

In this section, a different type of controller for the SAPF is discussed based on the previous studies. Synchronous Reference Frame (SRF) Theory is applied for the SAPF to compensate for current harmonics generated by the non-linear loads [7]. This control technique transforms a three-phase quantity into two-phase quantities to solve the network's harmonic compensation, resulting in a major reduction in Total Harmonic Distortion (THD) [8]. To

extract the current harmonics, the self-tuning approach technique is applied to overcome the problem of conventional harmonics compensation techniques which are based on the low pass or high pass filters [9]. For the mitigation of power quality issues, SAPF control techniques are applied in the distribution network. An active filter control technique offers superior performance compared to a conventional filter network and is also highly adaptable to the reduction of voltage and current harmonics as well [10]. The harmonic reduction ability of the SAPF purely depends on the reactive power detecting scheme, current harmonics, and compensation control algorithms [11]. To compensate for current harmonics generated by the non-linear load, Proportional Integral (PI) controller is applied. The PI controller has some drawbacks unable to the reduction of dynamic error and manual tuning control parameters and unsatisfactory harmonics compensation [12]. A predictive deadbeat PI-based control is investigated for the SAPF applications which result in a better harmonic reduction in a distribution network [13]. In [14], the Kalman filter-based PI controller is presented for improving the power quality issues but the design of the Kalman filter is under the steady-state and dynamic model behavior. But, handling uncertainty in the system is very difficult; it is necessary to design robust controllers [15]. To handle the uncertainty and disturbances due to the nonlinear distribution network, a robust controller playing the important role in nonlinear applications. In [16], H_∞ the controller is investigated for the regulation of current in three-phase SAF applications. This controller is enriching the power quality issues and more robustness. Human knowledge-based controllers, such as fuzzy logic and neural network controllers, effectively control the reduction of harmonics produced by the nonlinear load. Fuzzy logic controller-based SAPF is designed for the compensation harmonic current and this

controller does not require a complex mathematical background [17]. Furthermore, the neural network-based controller also discussed enriching current harmonics generated by the nonlinear loads [18]. On the other hand typical, PID controllers are used for efficient control of SAPF, but they need precise control input with tiny tolerance in plant variations to obtain the optimal performance. The aforesaid problems are effectively handled by the IMC controller. From the literature survey, it is clear that the IMC controller is highly recommended for the nonlinear control system and is more robust compared to the other controllers. Hence, in this paper, IMC is proposed for the SAPF, and simulation results are validated by using MATLAB/Simulink. The system performance is analyzed in terms of THD and also validated through a stability analysis. For a better understanding of the IMC controller, the feedback controller topologies are described in Fig.1. (i) Basic Feedback controller (ii) plant model inset feedback path (iii) basic feedback controller with plant model (iv) Basic IMC controllers.

Contributions of the Paper

- ✓ Internal model controller (IMC) is designed for the SAPF for the reduction harmonics generated by the nonlinear loads.
- ✓ The robustness of the IMC is examined through the stability analysis.
- ✓ The comparative analysis is made in terms of THD with others research outcomes.
- ✓ The simulation results of IMC are verified through MATLAB/Simulink.

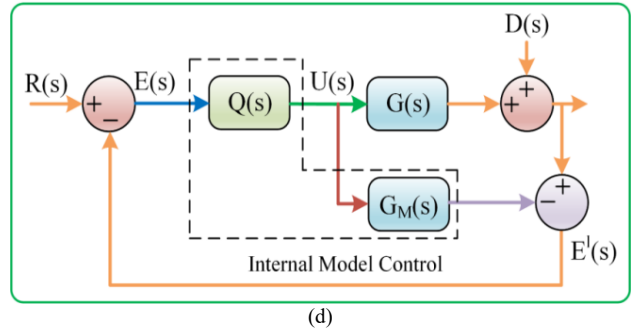
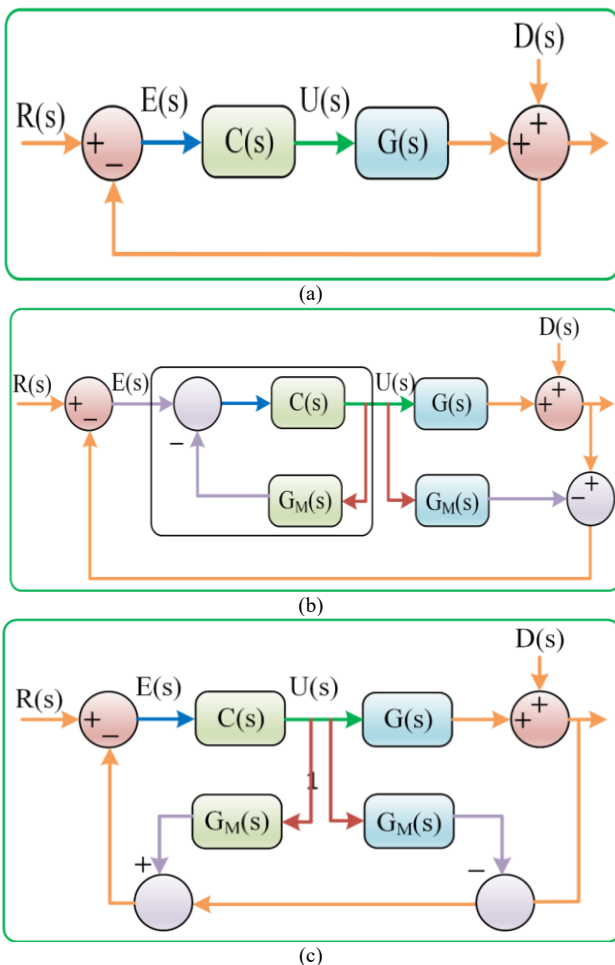


Fig.1. Configuration of feedback controllers: (a) classic (b) basic feedback (c) plant inserted in feedback (d) Internal model control

2. Shunt Active Filter configuration

The structure of the SAPF is shown in Fig.2 which consists of two main parts (i) shunt active filter section and non-linear load sections. Due to the connection of non-linear load such as traction and furnaces, the power system network is affected by the following parameters poor voltage regulation, harmonic injection to the power system network and it leads to lower power factor unbalancing as well. The voltage imbalance has an impact on the performance of other loads, especially squirrel-cage induction motors. To overcome the shortcomings above problems and improve the system efficiency, the different types of compensation networks can be applied to the power system network. To compensate for the current harmonic caused by such loads passive filter or active filter can be applied. In this paper, a SAPF based on the IMC is designed to minimize harmonics and balance non-linear loads. By injecting a variable magnitude current in quadrature with the line voltage, this SAPF can inject reactive power into the power system. From Fig. 2, by applying Kirchoff current law at the point PCC, the source current (I_s) is equal to the load current which is described

$$I_s = I_L$$

The load current is consists of two current components namely fundamental current components (I_{LL}) and harmonic current components (I_H) which are generated by the load. Due to the impact of the harmonic current components, the source current (I_s) is distorted and it is not in phase with source voltage (V_s).

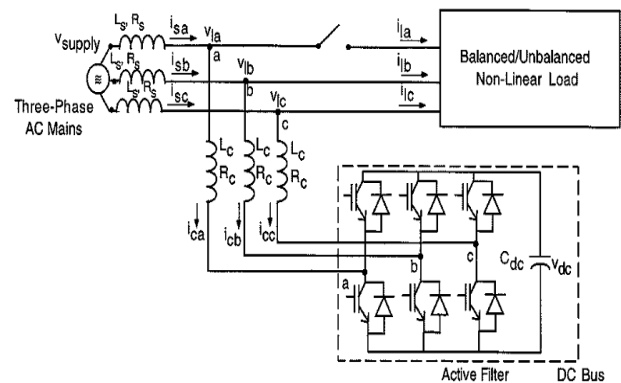


Fig. 2. Structure of shunt active power filter

To eliminate the effects of harmonic current, the SAPF is necessary. To improve the power quality, there are two

currents are generated. One current is cancellation of harmonic current components (I_H) and another current for regulation of constant dc-link voltage. The first injected current is equal to phase and magnitude. Furthermore, the injected current is opposite to the (I_H) components for the cancellation of I_H . The second current is used to maintain the constant dc-link voltage across the dc link. By maintaining constant dc-link voltage, the current injected at the PCC is equal to the I_H . Then injected current cancels out the fundamental harmonic current. Now source current becomes

$$I_s = I_{1L} + I_{dc}$$

Using a simple and new control system, this work presented how to use a SAPF for ac voltage regulation at load terminals (at PCC), harmonic elimination, power factor correction, and load balancing of nonlinear loads. Power-factor correction (unity), harmonic removal, power-factor correction, and load balancing of nonlinear loads have all been added to the SAPF's control scheme. The SAPF's control system has been improved to allow for power-factor correction (unity), harmonic removal, and load balancing of nonlinear loads. The proposed control algorithm automatically generates a self-supporting SAPF dc bus.

2.1 Modeling of SAPF

The 3-phase voltage and currents are transformed to evaluate the balanced three-phase device more conveniently by abc to dq0 transformation through a synchronous revolving frame. The dq-frame is revolving with a reference axis angle i.e., $\theta = \omega t$ from the abc-reference frame. The transformation from the d and q coordinates step variables are given as follows:

$$\begin{bmatrix} V_d \\ V_q \\ V_o \end{bmatrix} = K \begin{bmatrix} V_a \\ V_b \\ V_c \end{bmatrix} \quad (1)$$

Where

$$K = \sqrt{\frac{2}{3}} \begin{bmatrix} \cos\theta & \cos\left(\theta - \frac{2\pi}{3}\right) & \cos\left(\theta + \frac{2\pi}{3}\right) \\ \sin\theta & \sin\left(\theta - \frac{2\pi}{3}\right) & \sin\left(\theta + \frac{2\pi}{3}\right) \\ \frac{1}{\sqrt{2}} & \frac{1}{\sqrt{2}} & \frac{1}{\sqrt{2}} \end{bmatrix} \quad (2)$$

A linear mathematical model for each phase of the SAPF shown in Fig. 2 can be written as:

$$\left. \begin{aligned} L_f \frac{di_{fa}}{dt} &= -R_f i_{fa} + V_{fa} - V_{La} \\ L_f \frac{di_{fb}}{dt} &= -R_f i_{fb} + V_{fb} - V_{Lb} \\ L_f \frac{di_{fc}}{dt} &= -R_f i_{fc} + V_{fc} - V_{Lc} \end{aligned} \right\} \quad (3)$$

From eq. (2) and (3), equation (1) can be written in the following form:

$$L_f \frac{di_f}{dt} \begin{bmatrix} i_{fa} \\ i_{fb} \\ i_{fc} \end{bmatrix} = -R_f \begin{bmatrix} i_{fa} \\ i_{fb} \\ i_{fc} \end{bmatrix} + \begin{bmatrix} V_{fa} \\ V_{fb} \\ V_{fc} \end{bmatrix} - \begin{bmatrix} V_{La} \\ V_{Lb} \\ V_{Lc} \end{bmatrix} \quad (4)$$

dq-transformation from equation (4) is given by,

$$L_f \frac{di_f}{dt} \left(K^{-1} \begin{bmatrix} i_{fa} \\ i_{fb} \\ i_{fc} \end{bmatrix} \right) = -R_f K^{-1} \begin{bmatrix} i_{fa} \\ i_{fb} \\ i_{fc} \end{bmatrix} + K^{-1} \begin{bmatrix} V_{fa} \\ V_{fb} \\ V_{fc} \end{bmatrix} - K^{-1} \begin{bmatrix} V_{La} \\ V_{Lb} \\ V_{Lc} \end{bmatrix} \quad (5)$$

From the above eq.

$$\frac{d}{dt} K^{-1} = \omega \sqrt{\frac{2}{3}} \begin{bmatrix} -\sin\theta & \cos\theta & 0 \\ -\sin\left(\theta - \frac{2\pi}{3}\right) & \cos\left(\theta - \frac{2\pi}{3}\right) & 0 \\ -\sin\left(\theta + \frac{2\pi}{3}\right) & \cos\left(\theta + \frac{2\pi}{3}\right) & 0 \end{bmatrix} \quad (6)$$

$$K \frac{d}{dt} K^{-1} = \omega \begin{bmatrix} 0 & 1 & 0 \\ -1 & 0 & 0 \\ 0 & 0 & 0 \end{bmatrix} \quad (7)$$

$$\frac{d\theta}{dt} = \omega \quad (8)$$

Applying all the above relations in eq. (5)

$$\frac{di_f}{dt} \begin{bmatrix} i_{fa} \\ i_{fb} \\ i_{fc} \end{bmatrix} = \begin{bmatrix} -\frac{R_f}{L_f} & \omega & 0 \\ -\omega & -\frac{R_f}{L_f} & 0 \\ 0 & 0 & -\frac{R_f}{L_f} \end{bmatrix} \begin{bmatrix} i_{fa} \\ i_{fb} \\ i_{fc} \end{bmatrix} + \frac{1}{L_f} \begin{bmatrix} V_{fa} \\ V_{fb} \\ V_{fc} \end{bmatrix} - \frac{1}{L_f} \begin{bmatrix} V_{La} \\ V_{Lb} \\ V_{Lc} \end{bmatrix} \quad (9)$$

The SAPF's output voltage can be written as

$$\begin{aligned} V_{fd} &= MV_{dc} \cos\alpha \\ V_{fq} &= MV_{dc} \sin\alpha \end{aligned} \quad (10)$$

Where M is a factor that relates the DC voltage to the peak phase-to-neutral voltage on the AC side; Vdc-DC-link voltage; α - phase angle a condition in which the SAPF output voltage is higher than the bus voltage

$$\frac{d}{dt} \begin{bmatrix} i_{fd} \\ i_{fq} \end{bmatrix} = \begin{bmatrix} -\frac{R_f}{L_f} & \omega & \frac{M \cos\alpha}{L_f} \\ -\omega & -\frac{R_f}{L_f} & \frac{M \sin\alpha}{L_f} \end{bmatrix} \begin{bmatrix} i_{fd} \\ i_{fq} \\ V_{dc} \end{bmatrix} - \frac{1}{L_f} \begin{bmatrix} V_{Ld} \\ V_{Lq} \\ V_{L0} \end{bmatrix} \quad (11)$$

Because of switching losses in the voltage source inverter, the DC-link capacitor voltage drops. SAPF will use the necessary amount of Utility source current to maintain a constant going voltage. The combination of the current $i_{c,abc}$, and the switching loss component $i_{loss,abc}$ are given by

$$i_{f,abc} = i_{c,abc} + i_{loss,abc} \quad (12)$$

SAPF is responsible for supplying the desired current components so that only the active current comes from the power source to the load.

2.2 Proposed Internal Model Control based PID Controller

IMC-based PID control is presented in Fig.3. It starts from the IMC layout as seen in Fig.3 the comparative point between model and process control can be transferred.

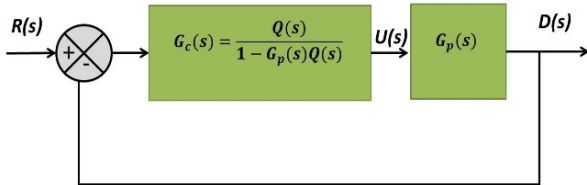


Fig.3. Block diagram of IMC-PID controller

3 The following steps are used in the IMC-based PID control system design.

Step 1: To make Q(s) proper or to give it derivative action, find the IMC transfer function, Q(s), which includes a filter, F(s). i.e. The numerator of q(s) has an order that is one higher than the denominator of Q. (s). This is a significant contrast from the IMC protocol. This can cause Q(s) to be improper in the IMC-based procedure to find an equivalent PID controller.

Step 2: Using the transformation, find the corresponding standard feedback controller.

$$G_c(s) = \frac{Q(s)}{1 - G_p(s)Q(s)} \quad (13)$$

write this in the form of a ratio between two polynomials

Step 3: By placing this in PID form and evaluating k_c , τ_i , τ_d . This procedure can often result in a PID controller with a lag term τ_f :

$$G_c(s) = k_c \left[\frac{\tau_i \tau_d s^2 + \tau_d s + 1}{\tau_d s} \right] \left[\frac{1}{\tau_f s + 1} \right] \quad (14)$$

Step 4: Closed-loop simulations can be carried out for both the perfect and mismatch model situations. The proposed SAPF is simulated in MATLAB/Simulink and the simulation parameters have been denoted in Table 1 and 2.

Table 1. Simulink Parameters of Power Supply and SAPF

Parameters of Source Power Supply	
Input Voltage	400 V
Supply Frequency	50 Hz
Source resistance (R _s)	0.1 Ω
Source Inductance (L _s)	1mH
Parameters of Shunt Active Power Filter (SAPF)	
IGBT Switch	600 V
Switching Frequency	10 kHz
DC link Capacitor	270μF
Resistance (R)	0.1Ω
Inductor (L _{sa} =L _{sb} =L _{sc})	10mH

Table 1 shows the MATLAB modeling parameters of power supply and SAPF. Squirrel cage induction motor, uncontrolled diode bridge rectifier with R-Load, and three-phase star-connected loads are all examined with the proposed SAPF configuration. In Table 2, the loads simulations parameters are mentioned.

Table 2. Simulink Parameters of Non-Linear Loads

Induction motor Parameters	
Machine type	Wound rotor
Power rating	4 KVA
Supply voltage	400 Volts
Frequency	50 Hz
Rated Speed	1500 RPM
Stator resistance	1.405 Ω
Stator Inductance	0.005839 H
Rotor resistance	1.395 Ω
Rotor Inductance	0.005839 H
Mutual Inductance (L _m)	0.1722 H
Parameters of 3-Phase Resistive Load	
Connection Type	Star connected
Resistance (R _a &R _c)	50 Ω
Resistance (R _b)	100 Ω
Uncontrolled Diode Bridge Rectifier	
Resistance (R _L)	50 Ω

4 Stability Analysis of the Proposed SAPF System

The stability of the proposed SAPF with and without IMC controller using Bode plot and Root-locus graph. The unfortunate gain and phase margins of the SAPF without IMC controller are shown in Fig.4. The system is unstable when the load disturbance occurs and the frequency of the system gets affected which is shown in Fig.5.

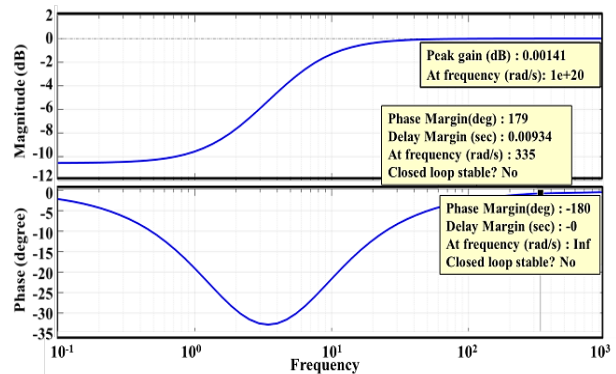


Fig.4. Bode plot of SAPF without IMC

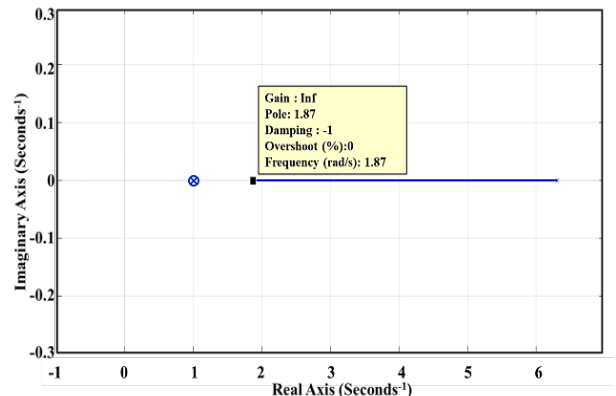


Fig.5. Root-locus of SAPF without IMC

The poles of the system are placed at the right side of the s-plane and the damping factor is -1. Hence, the system is unstable for the change in non-linear loading conditions. Incorporating the IMC system in the closed-loop control of SAPF increases the system stability which is verified using Bode and Root-locus graphs.

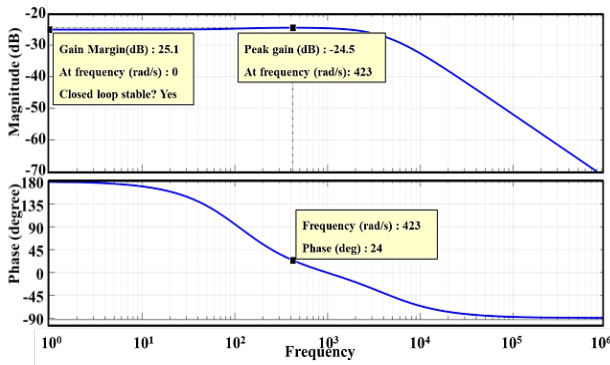


Fig.6. Bode plot of SAPF with IMC

In Fig. 4, the gain and phase margins of the system increased to 25.1 dB and 24 degrees respectively. Hence, the damping factor is +1 which ensures the closed-loop control system is highly stable as shown in Fig.6. The control of the system is analyzed with and without SAPF. The results have been compared for both conditions. The performances of the controller are verified at various loading conditions and their performance is analysed with respect to the THD.

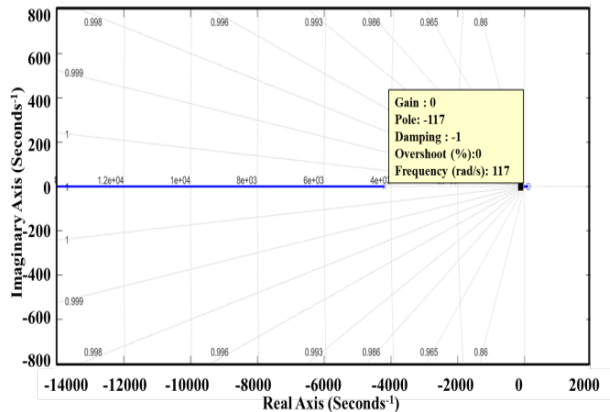


Fig. 7. Root-locus of SAPF with IMC

5. Simulation Results

The proposed SAPF comprises with three-phase supply system associated with the non-linear loads such as Squirrel cage induction motor, Diode bridge rectifier, and star-connected load. Due to the non-linear load characteristics, the system will draw different currents from the system. This non-linear load also injects the harmonics into the system as shown in Fig.7. This will lead to poor power factors at the source. Thus the additional sources connected to the distorted source will also have less power factor and harmonics. Moreover, the entire power will be lost in the form of heat. Heat is increased due to Iron & Copper losses at the harmonic frequencies and pulsating torque. Hence, the entire system will oscillate with non-linear load characteristics.

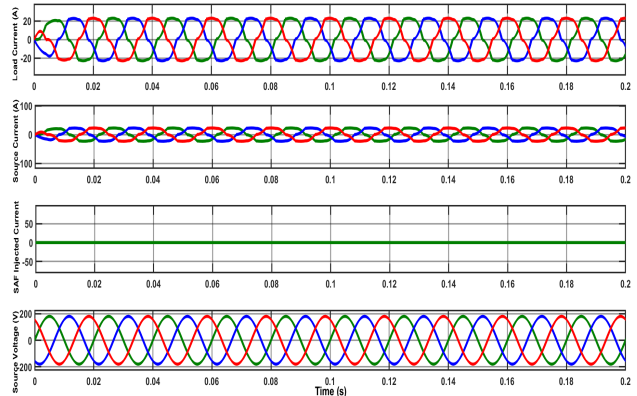


Fig. 7. Voltage and current waveforms at PCC without SAPF and IM-PID

The THD performance of the proposed system without a SAPF is indicated in Fig.8. From the harmonic spectrum, it is clear that there is no even order harmonic presented in this system. So the effect of even-order harmonic vanishes. But it contains a THD of 7.89% as indicated in Fig.8. The entire system has 7.89 % THD on both sides of sending end and receiving end. This THD can be eliminated to the standard level to improve the power quality of the system. SAPF with control arrangement is introduced to meet all the requirements in all aspects.

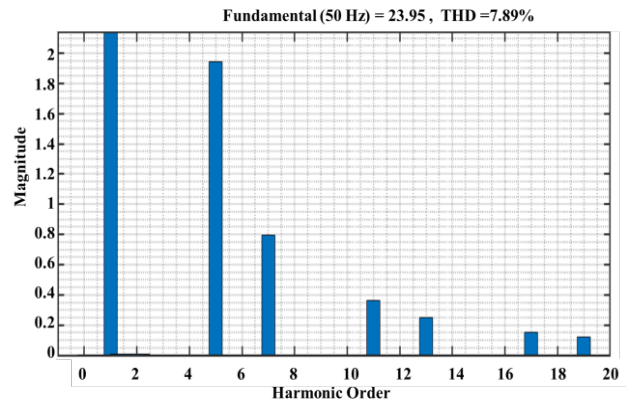


Fig. 8. Harmonic spectrum for non-linear load without SAPF

Similarly, load transients during 0.2 to 0.3 seconds as illustrated in Fig.9, the THD level is very high due to the sudden disturbance and non-linear load. The THD is increased to 12.57% during this incident as shown in Fig.10. Hence, the SAPF is required to compensate the current magnitude under non-linear and change in load conditions.

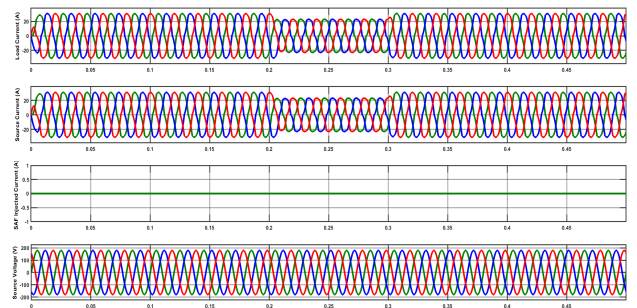


Fig. 9. Voltage and current waveforms at PCC without SAPF under load transients

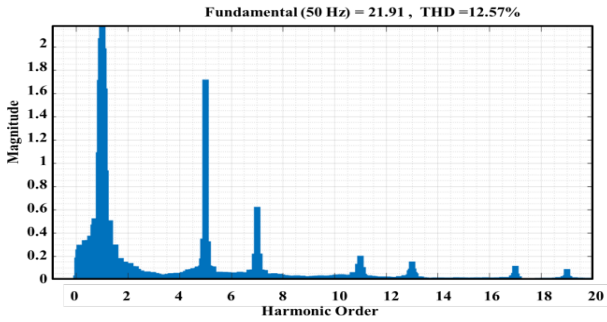


Fig. 10 Harmonic spectrum for Non-linear Load under transients without SAPF

A shunt active power filter is introduced in between source and load as shown in Fig. 11. To maintain better voltage regulation and power factor simple control technique is introduced. This control circuit will generate the necessary duty cycle to the shunt active power converter as shown in Fig.11. By controlling the duty cycle to the converter the harmonics present in the system for the non-linear loads can be eliminated and maintained at a standard level. The control circuit topology is shown in Fig.12.

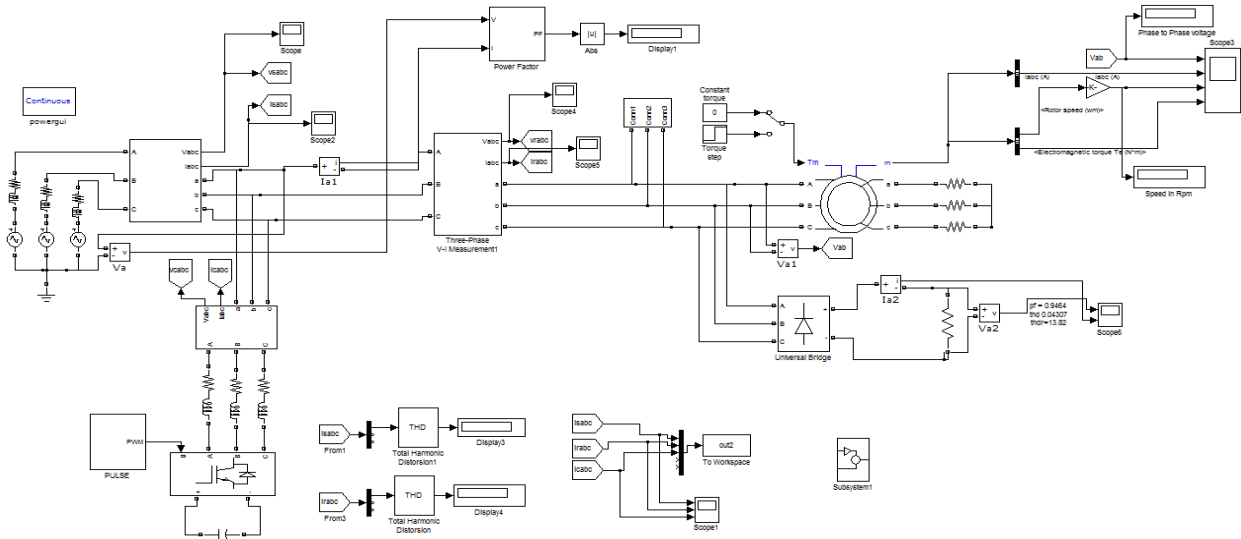


Fig.11 Non-linear loads with SAPF and IMC-PID control

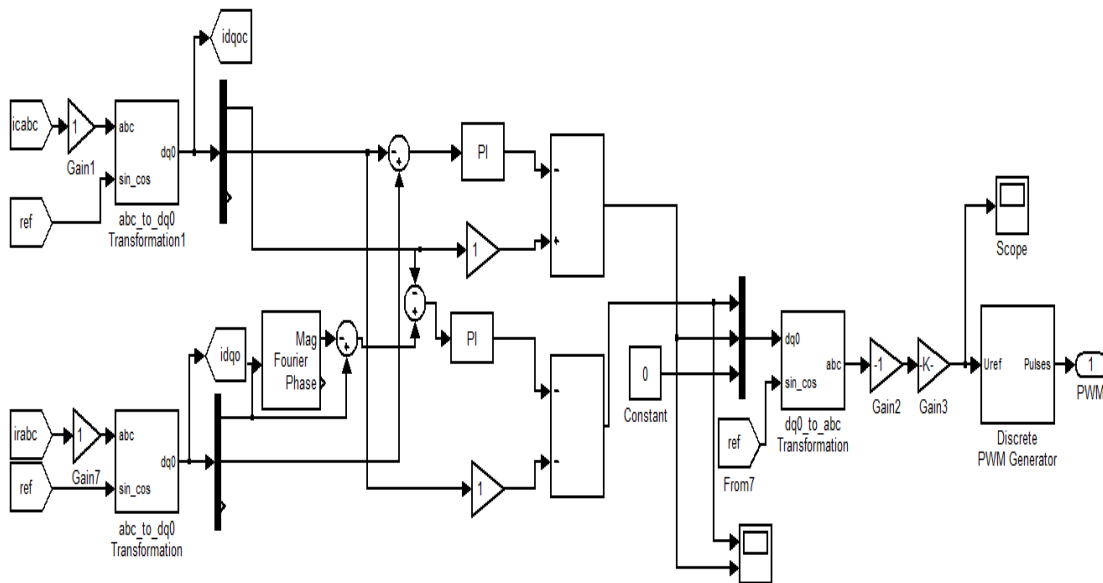


Fig.12. Control circuit topology

In this control method, a PWM pulse is generated to control the Shunt Active Filter (Inverter). The current has been taken from the receiving end (Load Current) and Shunt converter. Both three-phase currents have been converted into dq0 axis currents. This dq0- axis indicates the active, reactive, and reference components of the three-phase currents respectively. To understand the performance of the controller and SAPF, the load variations are created in the

different intervals in the simulation model. The difference inactive components from the load current and shunt converter current have been compared with the difference in reactive components of both converter and load currents. This comparison will provide the available active and reactive component currents. The PWM signal is generated by converting this resultant dq0 component into a three-phase (abc) component. This three-phase (abc) component is

converted into a PWM signal by using a discrete PWM block. The PWM signal of 10 kHz frequency is indicated in the figure. This signal is used for the control of the SAF converter to inject compensation current. This will provide voltage stability and also eliminate the Harmonics from the proposed system.

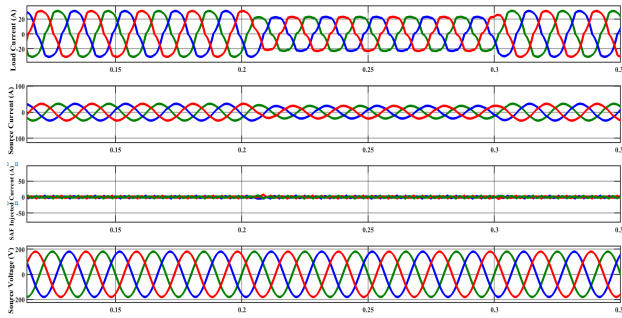


Fig. 13. Voltage and Current waveforms at PCC with SAPF and IMC-PID

Fig.13 shows the sudden variation in the load and corresponding load and current waveform in connection with the SAPF injected current. A total of 25 Amps load is considered for the analysis and 10 Amps load is disconnected during 0.2 to 0.3 sec as shown in Fig.13.

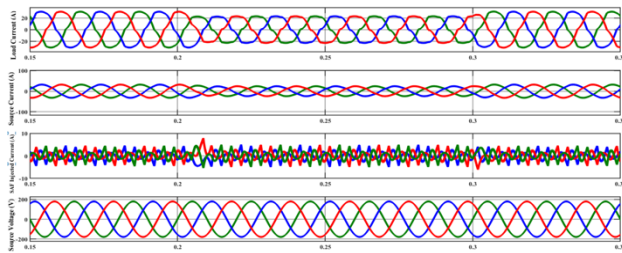


Fig. 14. Voltage and current waveforms during 0.15 to 0.35 sec with SAPF and IMC-PID

The SAPF finds the suitable compensation current and is aligned with the load current as shown in Fig.14 to maintain the source current closer to sinusoidal. The THD is also reduced to 3.50% and results are shown in Fig.15.

Similar to nonlinear load, unbalanced loads are considered in the simulation analysis. Fig.16 shows the sudden variation in phase a, b, and c load and corresponding load and current waveform in connection with the SAPF injected current. A total of 30 Amps load is considered for the analysis and 10 Amps load is disconnected during 0.2 to 0.3 sec as shown in Fig.16.

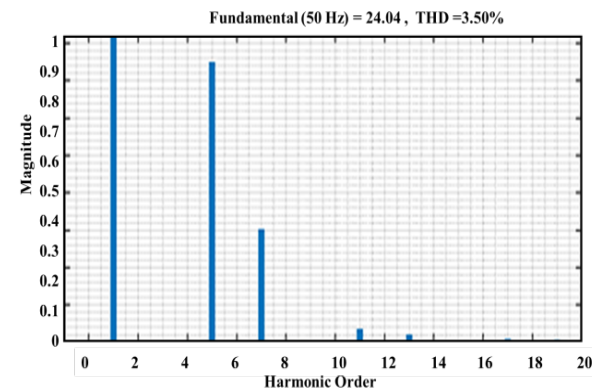


Fig. 15. Harmonic spectrum for Non-linear Load with SAPF

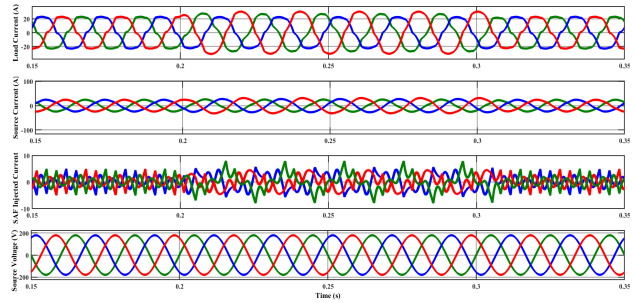


Fig. 16. Voltage and current waveforms at PCC with SAF and IMC-PID during unbalanced load

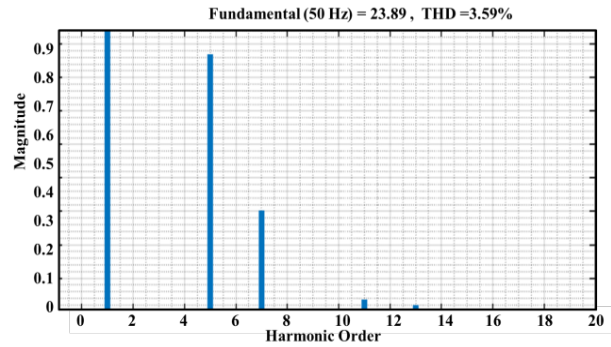


Fig. 17. Harmonic spectrum for non-linear unbalance Load with SAPF

The SAPF identifies the right balance current to keep the source current more proximal to the sinusoidal and is aligned with the charging current as shown in Fig.16. The THD is decreased to 3.59% as well, with results shown in Fig.17. By using the shunt Active Filter with proposed control strategies can effectively control the harmonics in both balance and unbalanced loading conditions. This proposed system mainly concentrated on the harmonic reduction of the three-phase shunt active filter is discussed. For the harmonic analysis, the system is considered with compensation and without compensation. The harmonic generated in [19], 23.80% without compensation and 3.80% with compensation using Artificial Neural Network (ANN). The harmonics reduction by using coordinated control (CC) based SAPF which produces 33.0% without compensation and 3.5% with compensations. 3.88 % of THD is produced by the conventional PI controller. The proposed IMC-based SAPF is examined both nonlinear balanced load and nonlinear unbalanced load. This proposed controller is offering a fast response for both balanced and unbalanced conditions.

Table 3. Comparative analysis

References	Before compensation % THD	After compensation %THD
Proposed	12.57	3.50 (Balanced load) 3.59 (Unbalanced load)
[19]	23.80	3.80 (ANN)
[20]	33.0	3.5 (CC)
[21]	28.01	3.88 (PI)

From Table 3 the THD analysis of the different controllers, the THD of the proposed system is very less which is about 3.50% (Balanced load) and 3.59% (Unbalanced load). Hence, the proposed system generates the THD within recommended IEEE-519 standard.

5 Conclusion

A three-phase Shunt Active Filter (SAFP) based on the Internal Model Controller (IMC) has been designed for the reduction of harmonics generated by the non-linear load. The main motivation of the paper is to design an IMC controller and stability analysis of three-phase SAFP controlled by an IMC controller. As a contrast to the other scientific findings, SAFP supported a better performance in terms of THD. In contrast, an internal model controller is used to assess the system's stability. Total Harmonic Distortion (THD) with and without compensation has been used to evaluate the system's performance. From simulation results, it is clear that THD generated by the proposed IMC was within the recommended standard of IEEE-519. A complete system is modeled and verified through MATLAB/Simulink. Research outcomes are as follows:

- ✓ Internal model controller (IMC) was designed for the SAFP for the mitigation of harmonics generated by the non-linear loads with balanced and unbalanced conditions.
- ✓ The robustness of the IMC has been examined through the stability analysis with different conditions.
- ✓ A comparative analysis is made in terms of THD with research outcomes and the simulation results are verified through MATLAB/Simulink.

This is an Open Access article distributed under the terms of the Creative Commons Attribution License.



References

1. AM. Eltamaly, Y. S. Mohamed, A-H. M. El-Sayed, M. A. Mohamed, N. A. Elghaffar, "Power quality and reliability considerations of photovoltaic distributed generation," *Technology and Economics of Smart Grids and Sustainable Energy*, 5(1), pp. 1-21, (2020).
2. T. Tran, D.Raisz, A. Monti, "Harmonic and unbalanced voltage compensation with VOC-based three-phase four-leg inverters in islanded microgrids," *IET Power Electronics*, 13(11), pp. 2281-2292, (2020).
3. TMT. Thentral, K. Vijayakumar, S. Usha, R. Palanisamy, T. S. Babu, H. H. Alhelou, A. Al-Hinai, "Development of Control Techniques Using Modified Fuzzy Based SAFP for Power Quality Enhancement," *IEEE Access*, 9, pp. 68396-68413, (2021).
4. SG. Basha, V. Mani, S. Mopidevi, "Single-phase thirteen-level dual-boost inverter based shunt active power filter control using resonant and fuzzy logic controllers," *CSEE Journal of Power and Energy Systems*, (2020).
5. A. Baliyan, M. Jamil, M. Rizwan, I. Alsaidan, M. Alaraj, "An intelligent PI Controller-based hybrid Series active power filter for power quality improvement," *Mathematical Problems in Engineering*, (2021).
6. Y. Hoon, M. A. MohdRadzi, M. A. A. MohdZainuri, M. A. MdZawawi, "Shunt active power filter: A review on phase synchronization control techniques," *Electronics*, 8(7), pp. 1-20, (2019).
7. EA. Al-Ammar, A. UIHaq, A. Iqbal, W. Ko, Marium Jalal, M. Almas Anjum, Hyeong-Jin Choi, Hyun-Koo Kang, "Synchronous reference frame theory based intelligent controller for current THD reduction," *Journal of Electrical Engineering & Technology*, 16(6), pp. 2917-2936, (2021).
8. R. Kumar, HO. Bansal, "Shunt active power filter: current status of control techniques and its integration to renewable energy sources," *Sustainable Cities and Society*, 42, pp. 574-592, (2018).
9. AA. Imam, R. Sreerama Kumar, Y. A. Al-Turki, "Modeling and simulation of a PI controlled shunt active power filter for power quality enhancement based on PQ theory," *Electronics*, 9(4), pp. 1-17, (2020).
10. H. Singh, M.Kour, D. V.Thanki, P. Kumar, "A Review on Shunt Active Power Filter Control Strategies," *International Journal of Engineering & Technology*, 7(4.5), pp. 121-125, (2018).
11. N. Malla, U.Tamrakar, D. Shrestha, Z. Ni, R. Tonkoski, "Online learning control for harmonics reduction based on current controlled voltage source power inverters," *IEEE/CAA Journal of Automatica Sinica*, 4(3), pp. 447-457, (2017).
12. AA. Imam, R. Sreerama Kumar, Y. A. Al-Turki, "Modeling and simulation of a PI controlled shunt active power filter for power quality enhancement based on PQ theory," *Electronics*, 9(4), pp. 1-17, (2020).
13. R. Zahira, A. P.Fathima, "A technical survey on control strategies of active filter for harmonic suppression," *Procedia Engineering*, 30, pp. 686-693, (2012).
14. R. Panigrahi, B.Subudhi, "Performance Enhancement of shunt active power filter using a kalman filter-Based H_{∞} control strategy," *IEEE Transactions on Power Electronics*, 32(4), pp. 2622-2630, (2016).
15. JH. Urrea-Quintero, N. Muñoz-Galeano, J. M. López-Lezama, "Robust control of shunt active power Filters: A dynamical model-based approach with verified controllability," *Energies*, 13(23), pp. 6253, (2020).
16. Y. Bekakra, L.Zellouma, Om Malik, "Improved predictive direct power control of shunt active power filter using GWO and ALO-Simulation and experimental study," *Ain Shams Engineering Journal*, (2021).
17. EM. Thajeel, M. M. Mahdi, EI. Abbas, "Fuzzy logic controller based Shunt Active Power filter for current harmonic compensation," In *2020 International Conference on Computer Science and Software Engineering (CSASE)*, pp. 94-99, (2020).
18. K.R. Sugavanam, K. M.Sundaram, R. Jeyabharath, P. Veena, "Convolutional neural Network-based harmonic mitigation technique for an adaptive shunt active power filter," *Automatika*, 62(3-4), pp. 471-485, (2021).
19. C.S. Subash Kumar, P. Rajasekar, M. Sathiyathan, M.Venkatesan, "FPGA Implementation of optimum switching angle control for shunt active filter using ANNSVPWM," *International Journal of Electronics*, DOI: 10.1080/00207217.2021.1972472
20. J. He, B. Liang, YW Li, C. Wang, "Simultaneous microgrid voltage and current harmonics compensation using coordinated control of dual-interfacing converters," *IEEE Transactions on Power Electronics*, 32(4), pp. 2647-2660, (2016).
21. A. Sakthivel, P. Vijayakumar, A. Senthilkumar, L. Lakshminarasimman, S. Paramasivam, "Experimental investigations on ant colony optimized PI control algorithm for shunt active power filter to improve power quality," *Control Engineering Practice*, 42, pp. 153-169, (2015).